# THE LONG-TERM EVOLUTION OF MULTILOCUS TRAITS UNDER FREQUENCY-DEPENDENT DISRUPTIVE SELECTION

G. Sander van Doorn[1,2] and Ulf Dieckmann[3,4]

[1]*Centre for Ecological and Evolutionary Studies, University of Groningen, Kerklaan 30, 9751 NN Haren, The Netherlands*
[3]*Evolution and Ecology Program, International Institute for Applied Systems Analysis, Schlossplatz 1, 2361 Laxenburg, Austria*
[4]*Section Theoretical Biology, Institute of Biology, Leiden University, Kaiserstraat 63, 2311 GP Leiden, The Netherlands*

*Abstract.*—Frequency-dependent disruptive selection is widely recognized as an important source of genetic variation. Its evolutionary consequences have been extensively studied using phenotypic evolutionary models, based on quantitative genetics, game theory, or adaptive dynamics. However, the genetic assumptions underlying these approaches are highly idealized and, even worse, predict different consequences of frequency-dependent disruptive selection. Population genetic models, by contrast, enable genotypic evolutionary models, but traditionally assume constant fitness values. Only a minority of these models thus addresses frequency-dependent selection, and only a few of these do so in a multilocus context. An inherent limitation of these remaining studies is that they only investigate the short-term maintenance of genetic variation. Consequently, the long-term evolution of multilocus characters under frequency-dependent disruptive selection remains poorly understood. We aim to bridge this gap between phenotypic and genotypic models by studying a multilocus version of Levene's soft-selection model. Individual-based simulations and deterministic approximations based on adaptive dynamics theory provide insights into the underlying evolutionary dynamics. Our analysis uncovers a general pattern of polymorphism formation and collapse, likely to apply to a wide variety of genetic systems: after convergence to a fitness minimum and the subsequent establishment of genetic polymorphism at multiple loci, genetic variation becomes increasingly concentrated on a few loci, until eventually only a single polymorphic locus remains. This evolutionary process combines features observed in quantitative genetics and adaptive dynamics models, and it can be explained as a consequence of changes in the selection regime that are inherent to frequency-dependent disruptive selection. Our findings demonstrate that the potential of frequency-dependent disruptive selection to maintain polygenic variation is considerably smaller than previously expected.

*Key words.*—Adaptive dynamics, evolutionary branching, Levene model, maintenance of genetic variation, population genetics, protected polymorphism, symmetry breaking.

Frequency-dependent selection plays an important role in the origin and maintenance of genetic variation (Felsenstein 1976; Slatkin 1979; Hedrick et al. 1976). Conditions for stable polymorphisms are much relaxed when fitness values are not constant but vary with the frequency of different genotypes present in a population. Protected polymorphisms can then be established whenever rare genotypes have a selective advantage (Lewontin 1958). This may even lead to situations in which, at population genetic equilibrium, the heterozygote resulting from an allelic dimorphism experiences a fitness disadvantage. (Note that this is the exact opposite of the situation required for stable polymorphisms to occur with constant fitness values.) In such a case, the population is caught at a fitness minimum, at which it experiences disruptive selection.

The consequences of such frequency-dependent disruptive selection have most extensively been investigated in the context of quantitative genetics (e.g., Slatkin 1979; Bulmer 1980) and in the related frameworks of evolutionary game theory (e.g., Maynard Smith 1982; Hofbauer and Sigmund 1998) and adaptive dynamics (e.g., Dieckmann and Law 1996; Metz et al. 1996; Geritz et al. 1998; Hofbauer and Sigmund 1998). See Abrams (2001) for a comparison of these three methods. Although the insights obtained through these different approaches are similar in some respects (Taylor 1996), their predictions for the effects of frequency-dependent disruptive

selection are strikingly different. In quantitative genetics models, the maintenance of genetic variation results from the broadening of continuous phenotypic distributions exposed to such selection. In adaptive dynamics models, frequency-dependent disruptive selection can cause evolutionary branching (Metz et al. 1996; Geritz et al. 1997, 1998). Such branching processes characteristically involve the convergence of a monomorphic population to a fitness minimum, followed by the adaptive emergence and further diversification of a discrete polymorphism.

The discordance of these predictions is caused by the different genetic assumptions underlying quantitative genetics and adaptive dynamics models. Quantitative genetics models are often purely phenomenological, but when a mechanistic underpinning is given, it is usually assumed that phenotypic characters are influenced by a large number of loci, each of which contributes only marginally to the phenotype. In every generation, the genetic variation present in the parent generation is redistributed among the offspring through recombination and segregation, that is, as a consequence of sexual reproduction. Because many loci are involved in this process, the distribution of phenotypes in the population is continuous and normal. Adaptive dynamics models, in contrast, usually consider asexual reproduction (or single-locus, haploid genetics) and monomorphic populations (for exceptions see Kisdi and Geritz 1999; Van Dooren 1999).

From the viewpoint of population genetics, the assumptions of infinite loci with infinitesimal effects (quantitative genetics) or of asexual reproduction (adaptive dynamics) are both highly idealized. It is therefore difficult to predict the

---

[2] Present address: Section of Integrative Biology, University of Texas, 1 University Station C0930, Austin, Texas 78712; E-mail: vandoorn@santafe.edu.

effect of frequency-dependent disruptive selection for realistic genetic settings. Despite the fact that frequency-dependent selection has been included in the theory of population genetics right from its conception (Fisher, 1930), most of population genetics theory assumes constant fitness values (for exceptions see Clarke 1972; Cockerham et al. 1972; Cressman 1992); such theory cannot be used to predict the consequences of frequency-dependent selection. In particular, the evolutionary dynamics of multilocus characters under frequency-dependent disruptive selection remains elusive. However, several attempts have been made to bridge the gap between population genetic and phenotypic models of frequency-dependent selection, and particularly the integration of population genetics with evolutionary game theory has received considerable attention (e.g., Cressman, 1992; Hofbauer and Sigmund 1998).

As a case in point, Bürger (2002a,b) presented a population genetic analysis of a model of intraspecific competition that had previously been analyzed within both the quantitative genetics (e.g., Slatkin 1979) and the adaptive dynamics framework (e.g., Metz et al. 1996). Bürger focused on the dynamics and population genetic equilibria of the frequencies of a fixed set of alleles in a multilocus model with frequency-dependent disruptive selection. He investigated the conditions under which disruptive selection on the phenotypes can be observed and quantified the amount of genetic variation that can be maintained. The analyzed model exhibits a number of unexpected phenomena, which underscore that the population genetics of frequency-dependent disruptive selection can be surprisingly complex.

A complementary approach was initiated by Kisdi and Geritz (1999) and Van Dooren (1999), who extended adaptive dynamics models by incorporating diploid genetics and sexual reproduction. Focusing on the simplest model of interest, these authors studied the evolution of alleles at a single locus under frequency-dependent disruptive selection. Unlike models that consider a fixed and limited set of alleles, these analyses explicitly considered mutations with small phenotypic effects. Long-term evolution can then proceed as a sequence of substitution steps during which existing alleles are replaced by novel ones created by mutation. Similar approaches have been developed in the population genetics literature (e.g., Keightley and Hill 1983; Bürger et al. 1989). As in asexual adaptive dynamics models, frequency-dependent disruptive selection can cause evolutionary branching in diploid sexual populations (this occurs under the same conditions as in asexual models), leading to the establishment of a polymorphism of alleles (Kisdi and Geritz 1999). As a consequence of the constraints imposed by random mating and segregation, the evolution of dominance-recessivity relations between the alleles is selectively favored (Van Dooren 1999).

In this paper, we aim to extend the understanding of the long-term consequences of frequency-dependent disruptive selection by analyzing mutations and allele substitutions in a multilocus model. This approach extends the earlier work of Bürger (2002a,b) by allowing for long-term evolution by mutations and allele substitutions. At the same time, our work extends the analysis by Kisdi and Geritz (1999) by allowing for multilocus genetics. We will consider Levene's soft-selection model (Levene 1953) as a prototypical example of situations generating frequency-dependent disruptive selection. Levene's model is commonly used for studying the maintenance of variation in a heterogeneous environment; it is relatively simple, its population genetics are well known (Roughgarden 1979), and it has been considered in several related studies (Kisdi and Geritz 1999; Van Dooren 1999; Spichtig and Kawecki 2004).

## MODEL DESCRIPTION

### Ecological Assumptions

We consider an organism with discrete, nonoverlapping generations in a heterogeneous environment consisting of two habitats. Individuals are distributed at random over the two habitats at the start of each generation. The two habitats differ in ecological conditions such that an individual is more or less adapted to a habitat depending on its ecological strategy $z$, a one-dimensional quantitative character. Specifically, we assume that an individual's viability in habitat $i = 1, 2$ is given by

$$v_i(z) = \exp\left[-\frac{1}{2}(z - \mu_i)^2/\sigma^2\right],\qquad(1)$$

which implies that the optimal phenotype is $\mu_1$ in the first habitat and $\mu_2$ in the second. The parameter $\sigma$ is an inverse measure of the intensity of local selection and determines how rapidly viability declines with the difference between an individual's ecological strategy and the locally optimal one. Without loss of generality, we set $\mu_1 = -\mu_2 = \mu$.

We assume soft selection (sensu Levene 1953; see also Ravigné et al. 2004); in each generation, a fixed number $f_iN$ of randomly chosen adults are recruited from habitat $i$; throughout, we set $f_1 = f_2 = \frac{1}{2}$. These adults form a single mating population of population size $N$, in which mating occurs at random and offspring are produced at the end of each generation.

### Genetic Assumptions

The ecological strategy $z$ is encoded by $L$ diploid loci. One or more distinct alleles may occur at every locus. We use the index $k$ to arbitrarily label the different alleles that occur within the population at a specified locus $l$. Correspondingly, $a_{lk}$ denotes the $k$th allele at the $l$th locus, and $x_{lk}$ denotes its phenotypic effect (allelic effect). We initially assume that loci are unlinked and that alleles interact additively at each locus and between loci. Hence, for an individual carrying alleles $a_{lk'}$ and $a_{lk''}$ at the $l$th locus, the phenotypic effect of this locus is given by $y_l = x_{lk'} + x_{lk''}$, and the individual's ecological strategy is given by

$$z = \sum_{l=1}^{L} y_l.\qquad(2)$$

Later in this study, we will also consider nonadditive interactions within and between loci, as well as genetic linkage between loci.

Unlike previous models (reviewed in Felsenstein 1976; Hedrick et al. 1976), which were concerned with the short-term evolutionary process of changes in allele frequencies, we do not constrain the set of alleles that may be present in

the population. By allowing new alleles to appear through mutation, we can study the long-term evolutionary process of changes in the phenotypic effects of alleles. Mutations occur at rate $m$ per allele per generation and change the phenotypic effect of an allele by an amount drawn from a normal distribution with zero mean and standard deviation $\sigma_m$.

### Simulation Details

In addition to analytic approximations, we consider an individual-based model. At the start of a simulation, the population is initialized by creating $N$ identical individuals that are homozygous at all loci. Although the initial population exhibits no genetic variation, it usually takes just a few generations before mutation has created sufficient genetic variation for adaptive change to occur. The phenotypic effects of the alleles used to initialize the population is chosen such that the initial phenotype is far away from the average of the optimal phenotypes in the two patches. Other choices of the initial phenotype do not lead to different results: the population always first converges on the phenotype $z = 0$, the average of the patch optima, before further evolution occurs (see below).

At regular intervals, we determined the distribution of phenotypes in the population and the distributions of the phenotypic effects of alleles at individual loci.

### Environmental Variation

Throughout this paper and as indicated by equation (2), we maintain conceptual simplicity by supposing that the ecological strategy is completely genetically determined. However, effects of the microenvironment on the phenotype can be incorporated into the model straightforwardly by modifying the selection parameter $\sigma^2$ (Bürger 2000, pp. 158–160); it changes to $\sigma^2 + V_e$, where $V_e$ denotes the variance of the environmental component of phenotypic variation. The validity of this rescaling argument was confirmed by individual-based simulations (see Figure S1 in the supplementary material available online only at http://dx.doi.org/10.1554/06-291.1.s1).

It should be noted that variation in the environment itself, caused by, for instance, variability of the parameters $\mu$ and $\sigma$, cannot be dealt with simply by rescaling the model. For this reason, we have explored a small number of scenarios by means of individual-based simulations (for an example, see Figure S2 in the supplementary material available online); these simulations confirmed the robustness of our conclusions. A more comprehensive analysis of the effects of environmental variability on the maintenance of polygenic variation in the model analyzed here is suggested as an interesting topic of future research.

### Individual-Based Model

#### Two Selection Regimes

Our investigations of the individual-based model defined above show that, not unexpectedly, evolutionary outcomes critically depend on the relative magnitude of the parameters $\mu$ and $\sigma$.

When the optimal strategies in the two habitats are not too different, or when viability selection is weak ($\mu < \sigma$), long-term evolution of the ecological strategy $z$ proceeds toward the generalist strategy $z^* = 0$ (results not shown). Once the population has reached this generalist strategy, no further phenotypic evolution takes place. Mutation-selection balance maintains only a tiny amount of variation in the population. These observations agree with analytical results (Geritz et al. 1998; Kisdi and Geritz 1999) that predict the strategy $z^* = 0$ to be both convergence stable and evolutionarily stable for $\mu < \sigma$. The former implies that evolution through small phenotypic steps will proceed toward $z^* = 0$, with each step corresponding to the mutation and subsequent substitution of an allele. The latter implies that no allele coding for an alternative phenotype will be able to invade once the phenotype $z^* = 0$ has been established, and, therefore, that the population experiences stabilizing selection at $z^* = 0$.

By contrast, when the difference between the optimal strategies is large, or when viability selection is strong ($\mu > \sigma$), we observe the emergence of a stable phenotypic polymorphism through the process of evolutionary branching (Metz et al. 1996; Geritz et al. 1997, 1998). Figure 1 shows a simulation for $\mu = 1.5$ and $\sigma = 1.0$ (we performed simulations for $0.2 \leq \mu/\sigma \leq 2.0$ in steps of 0.2 and $2.0 \leq \mu/\sigma \leq 5.0$ in steps of 0.5). Other parameters are set to $N = 1000$, $L = 3$ (we also considered $L = 1, \ldots, 5, 10, 20, 50, 100, 250$), $\sigma_m^2 = 10^{-3}$, and $m = 10^{-4}$; unless stated otherwise, these parameter values will be used throughout this paper. As illustrated in the left panel of Figure 1, directional evolution first converges toward the generalist strategy $z^* = 0$, where selection turns disruptive. This is because the strategy $z^* = 0$ is convergence stable, but not evolutionarily stable (Geritz et al. 1998; Kisdi and Geritz 1999). Therefore, alleles coding for alternative phenotypes can invade the generalist population, thus establishing genetic and phenotypic polymorphism (middle and right panel).

### A General Pattern of Polymorphism Formation and Collapse

We find that establishment of this polymorphism follows a characteristic sequence of phases.

*Convergence.*—During phase 1 (Fig. 1, left panel; generations 0 to 10,000), the evolving population simply converges to the branching point through the gradual adjustment of phenotypic effects, without any significant between-locus or within-locus variation being built up. Phase 1 sets the stage for the establishment of the later polymorphism—by bringing about a regime of frequency-dependent disruptive selection—without yet itself contributing to that process.

*Symmetric divergence.*—In phase 2, which commences right after branching (Fig. 1, middle panel; generations 10,000 to 30,000), the phenotypic differentiation between alleles grows gradually, due to mutations and allelic substitutions. Closer inspection reveals that all loci become polymorphic during this phase. In particular, we observe two equally frequent, distinct classes of alleles with equal but opposite phenotypic effects at each locus. Moreover, the differences between the phenotypic effects of these classes of alleles are roughly equal for all loci. Consequently, the phenotype segregates as if it were determined by $L$ additive,
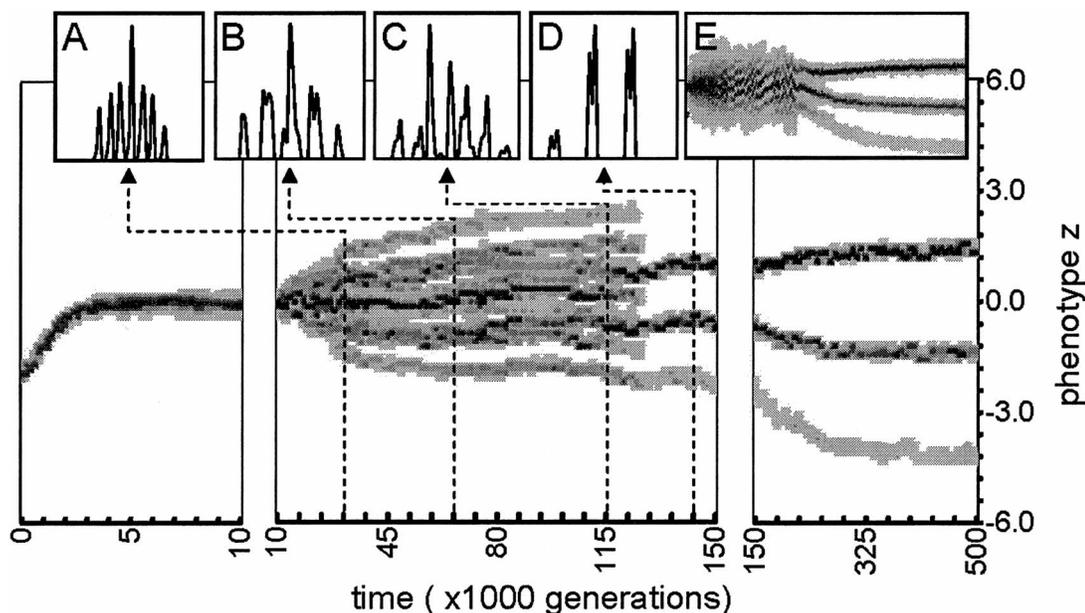
Fig. 1. Evolution in individual-based model. The three panels of this figure show the distribution of phenotypes during the rapid convergence to the evolutionary branching point (left), the subsequent phase of diversification at several loci (middle), and the final phase of evolution at a single locus (right). Small insets A–D show the frequency distribution (frequency is on the vertical axes) of phenotypes (on the horizontal axes) at four moments during the simulation (indicated by dashed lines). We also ran simulations with more than three loci: inset E shows an example for $L = 100$ loci (time, on the horizontal axis, extends to 500,000 generations; phenotype, on the vertical axis, ranges from $-5.0$ to $5.0$). Grayscales in the main figure and inset E indicate the frequency of phenotypes. At any moment in time, the most common phenotype is shown in black, while less common phenotypes are shown in lighter shades of gray. Note the different scales of the time axis in the three panels. Parameters as listed in the text.

diallelic, diploid loci, with identical pairs of alleles at all loci. Such genetic systems can give rise to $2L + 1$ different phenotypes, exactly the number of phenotypic classes we observe in our simulations (Fig. 1, inset A; $L = 3$ loci implies seven such classes).

*Between-locus symmetry breaking.*—In phase 3 (Fig. 1, middle panel; generations 30,000 to 125,000), phenotypic variation continues to increase until the distribution of realized phenotypes approximately covers the range from $-\mu$ to $\mu$. However, the symmetry between loci is broken during this phase. At some loci, the alleles continue to diversify, whereas at other loci the differentiation between alleles decreases or alleles are lost altogether (Fig. 1, inset B). Eventually, only one polymorphic locus remains. This effect was observed to occur independently of the number of loci encoding the ecological strategy (see Fig. 1, inset E, for a simulation with $L = 100$) and independently of the parameters $\mu$ and $\sigma$, as long as $\mu > \sigma$. At the remaining polymorphic locus, two classes of alleles give rise to three distinct classes of phenotypes (two homozygotes and a heterozygote; Fig. 1, inset D).

*Within-locus symmetry breaking.*—During phase 4 (Fig. 1, generations 125,000+), phenotypic effects and frequencies at the last polymorphic locus become asymmetric. This process has previously been studied by Kisdi and Geritz (1999), who showed that within-locus asymmetries evolve under a wide range of parameters. During phase 2, and essentially also during phase 3, the distinct classes of alleles at each particular locus have equal frequencies and opposite but equal effects on the phenotype, such that heterozygotes have phe-

notypic effects close to zero. During phase 4, this symmetry is lost, such that the heterozygote matches one of the two locally optimal phenotypes, with the other locally optimal phenotypes being matched by one of the homozygotes ($z \approx \mu$ and $z \approx -\mu$; Fig. 1, right panel). The remaining homozygote expresses a poorly adapted phenotype ($z \approx -3\mu$; Fig. 1, right panel). This makes it evident that the alleles carried by the latter homozygote (let us refer to its genotype as *aa*) have a larger phenotypic effect ($x_a \approx -3\mu/2$) than the alleles carried by the former homozygote (genotype *AA*; $x_A \approx -\mu/2$). The frequency of the allele *a* approaches ¼. This is because, at the time of mating, half of the population consists of individuals from the first habitat, where only *AA* individuals stand a fair chance of survival, while the other half consists of individuals from the second habitat, where only *Aa* individuals survive. In Figure 1, the asymmetry in the phenotype distribution primarily grows during phase 4 (inset D), but is already initiated to some slight extent during phase 3 (inset C). Beyond these final adjustments, the population's phenotypic and allelic composition remains stable.

Replicate simulations for the same set of parameters (at least 20 replicates per parameter condition) show no variation on the four-phase pattern described above. Also quantitatively, Figure 1 gives a representative impression of the timing of the different phases. We do observe some variation between replicates in the length of the phase of symmetric divergence, though. In about 10% of the replicates, between-locus symmetry breaking occurs at a premature stage, such that polymorphism may already be lost at one locus (or, oc-

casionally, at two loci) before phenotypic diversification has come to an end.

The parameters used for the simulations presented in Figure 1 lead to mutational heritabilities, $h_m^2 = 2Lm\sigma_m^2$, of $6 \times 10^{-7}$ (main figure) and $2 \times 10^{-5}$ (inset E), and genomic mutation rates, $U = 2Lm$, of $6 \times 10^{-4}$ (main figure) and $2 \times 10^{-2}$ (inset E). These values span the lower half of the estimated range of naturally realized values (e.g., Rifkin et al. 2005). For low values of $h_m^2$ and $U$ it takes considerable time until polygenic variation is lost. The whole evolutionary process occurs more rapidly when the mutational heritability is enlarged through an increase of the mutation rate, $m$ or of the variance of mutational effects, $\sigma_m^2$. However, more pronounced mutations make it more difficult to single out for further investigation the selection-driven component of evolutionary change; for that reason, we have typically assumed small values for $m$ and $\sigma_m^2$ (but see Fig. 7).

As we will demonstrate below, the four-phase pattern illustrated in Figure 1 is robustly observed in several variations of our basic model. While phases 1 and 4 already occur in single-locus models (Kisdi and Geritz 1999), in this paper we focus on the new patterns resulting from the symmetry breaking between loci during phase 3, and thus on processes that are unique to multilocus models.

## DETERMINISTIC MODEL

### Derivation of Deterministic Dynamics

We further investigate the observed loss of polymorphism at all but one locus by analyzing a deterministic approximation of our model. For this purpose we derived deterministic equations for the expected rate of evolutionary change in allelic effects, assuming that mutations are rare and their incremental effects are small. Directional evolution then proceeds by steps involving allelic mutation, invasion, and fixation (Metz et al. 1992, 1996; Dieckmann and Law 1996; Weissing 1996; Hofbauer and Sigmund 1998; Geritz et al. 2002). The outcome of a single step in this process, that is, whether or not a new mutant allele will be able to invade and substitute an existing resident allele, is determined by the invasion fitness of the mutant allele, that is, by the rate at which the frequency of the mutant allele increases when it is still rare (Metz et al. 1992, 1996). In a multilocus context, this quantity will depend on a combination of fitness effects of the mutant allele in the different genetic backgrounds created by other polymorphic loci (see appendix). Mutant alleles with positive invasion fitness have a chance to invade the resident population, and once they have overcome the threat of accidental extinction by demographic stochasticity (Dieckmann and Law, 1996; Metz et al. 1996), they will go to fixation (except under certain special and well-understood circumstances; Geritz et al. 2002). It can be shown that series of such substitution events result in gradual evolutionary change at a rate and in a direction that is related to the gradient of invasion fitness (Dieckmann and Law 1996).

We followed standard procedures for the derivation of invasion fitness and for the subsequent derivation of dynamical equations for the evolutionary rate of changes in allelic effects (Dieckmann and Law 1996; Kisdi and Geritz 1999; details are provided in the appendix).
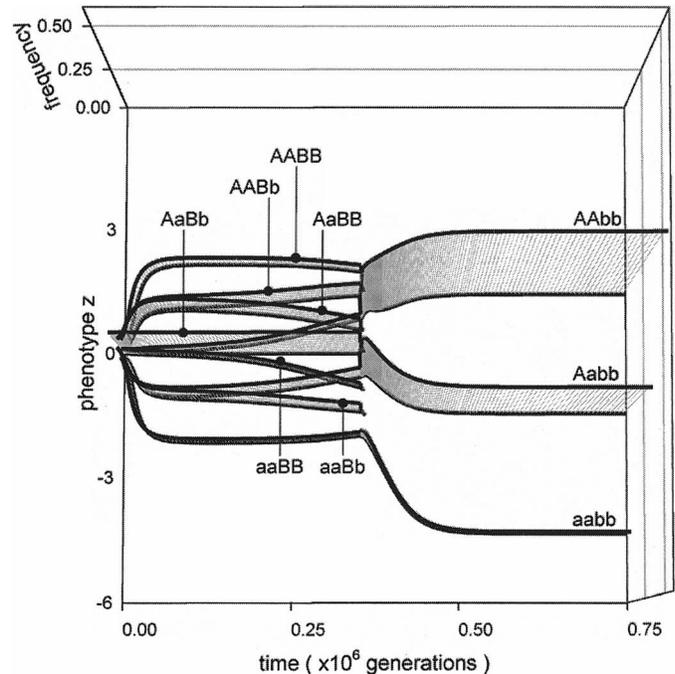


FIG. 2. Evolution in deterministic model. The deterministic approximation of our model tracks the phenotypic differentiation of alleles at two polymorphic loci. With two alleles at each locus (*A* and *a* at the first, *B* and *b* at the second locus), at most nine different classes of genotypes (indicated by the labels *AABB*, . . . , *aabb*) are present within the population at any moment in time. Individuals within the same class of genotypes have identical phenotypes. The phenotypes associated with each class of genotypes and their frequencies change over time, due to evolutionary change in the phenotypic effects of alleles. The time scale of this process may vary with parameters such as the mutation rate, the mutational variance, and the population size (see appendix). Parameters as in Figure 1.

### Illustration of Deterministic Dynamics

Numerical results for the deterministic model are shown in Figure 2. The simulation starts with a population located at the evolutionary branching point, just after a dimorphism has arisen at two loci. There are two alleles at the first locus, which we will refer to as *A* and *a,* and two alleles at the second locus, henceforth referred to as *B* and *b* (this does not imply that the alleles *A* and *B* are dominant; as before, alleles act additively on the phenotype).

Until about $1.0 \times 10^5$ generations, the phenotypic effects of the alleles at both loci diversify rapidly and symmetrically (corresponding to phase 2 as described above), giving rise to five phenotypic classes. The difference between the phenotypic effects of alleles *B* and *b* then diminishes gradually, until the allele *B* is suddenly lost at about $3.5 \times 10^5$ generations (phase 3), so that only three phenotypic classes remain (which of the two loci loses its dimorphism depends on arbitrarily small initial asymmetries between them). The difference between the phenotypic effects of alleles *A* and *a* continues to grow throughout phase 3. Finally (phase 4), the alleles at this locus evolve in such a way that one homozygote (*AA*) and the heterozygote (*Aa*) match the optimal phenotypes, whereas the remaining homozygote (*aa*) expresses a suboptimal phenotype. The frequency of the allele *a* then

declines to approximately 0.25. This is again explained by the fact that 50% of the mating population, that is, the part contributed by one habitat, will consist mainly of *AA* individuals, whereas the remaining 50% from the other habitat will mainly consist of *Aa* individuals. The alternative outcome also is possible, with the matches provided by *aa* and *Aa* instead (which of these two outcomes is realized depends on arbitrarily small initial asymmetries between the allelic effects at the remaining dimorphic locus).

Asymmetries in the initial conditions determine on what time scale symmetry breaking within and between loci will occur (asymmetries develop faster when the initial asymmetries are larger). Taking into account the expected value of initial asymmetries between alleles in the individual-based simulations, we find good quantitative agreement between both implementations of our model. Therefore, we use the deterministic model for further investigation.

### *Comprehensive Analysis of Deterministic Dynamics*

A comprehensive picture of the evolutionary dynamics of our model can be obtained by focusing on two-locus diallelic genetics (such as illustrated in Fig. 2) to study the underlying dynamics in allele space. Let us therefore denote the phenotypic effects of alleles *A, a, B,* and *b* as $x_A$, $x_a$, $x_B$, and $x_b$, respectively. Without loss of generality, we may define

$$x_A = \bar{x} + \delta_1 + \Delta, \tag{3a}$$

$$x_a = \bar{x} - \delta_1 + \Delta, \tag{3b}$$

$$x_B = \bar{x} + \delta_2 - \Delta, \quad \text{and} \tag{3c}$$

$$x_b = \bar{x} - \delta_2 - \Delta, \tag{3d}$$

such that $\bar{x}$ represents the average phenotypic effect of all four alleles, and $\delta_1$ and $\delta_2$ measure the phenotypic differentiation between alleles at the first and second locus, respectively. The quantities $\bar{x} + \Delta$ and $\bar{x} - \Delta$ then represent the average phenotypic effects of the alleles at the first and second locus, respectively. The variable $\bar{x}$ is indicative of the asymmetry between alleles at polymorphic loci, whereas the difference $\delta_1 - \delta_2$ relates to the asymmetry between loci. Because alleles interact additively within and between loci, the coefficient $\Delta$ has no effect at the phenotypic level, and hence is not subject to selection. This allows us to represent allele space in three dimensions.

Figure 3 illustrates the different equilibria we find in allele space. Starting from a population that is monomorphic at both loci ($\delta_1 = \delta_2 = 0$), evolution first converges to the evolutionary branching point (indicated as BP in Fig. 3). Any slight degree of dimorphism developing right at the branching point (or, alternatively, having been present initially), takes the population away from this point, toward an equilibrium at which a symmetric allelic dimorphism is established at both loci (equilibrium S2). This equilibrium is not stable, however. Further evolution proceeds toward an equilibrium at which only one locus supports a symmetric allelic dimorphism (equilibrium S1). Unless the difference between the patch optima is very large relative to the selection parameter σ (for the exact conditions, see Kisdi and Geritz 1999), this equilibrium is also not stable, such that the final phase of
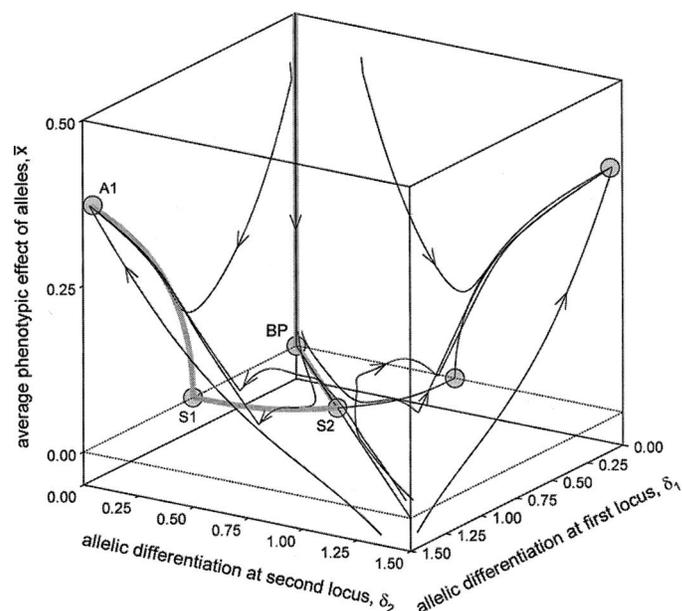


FIG. 3. Evolution in allele space. Simulations of the deterministic approximation of our model, started from various initial conditions, are represented as trajectories in allele space (black lines with arrows). The location of equilibria is indicated by gray circles. The location of equilibria and their stability properties were calculated numerically. The thick gray trajectory highlights how evolution proceeds toward the equilibrium A1 via the equilibria BP, S2, and S1 (for details see the main text). Notice that in this depiction trajectories may intersect with other trajectories, because there exist multiple population genetic equilibria for some combinations of alleles. Parameters as in Figure 1.

evolution involves the transition to an asymmetric allelic dimorphism at a single locus (equilibrium A1).

The sequential approach of an initial condition IC toward the equilibria BP, S2, S1, and A1 in Figure 3 can be recognized in the four different phases of the individual-based dynamics shown in Figure 1: IC → BP (phase 1), BP → S2 (phase 2), S2 → S1 (phase 3), S1 → A1 (phase 4). The four different phases are the more pronounced the closer trajectories stay to the itinerary IC → BP → S2 → S1 → A1 (see Fig. 3). Technically speaking, equilibria like BP, S1, and S2 are called saddle points. Such points are notorious for slowing down dynamics when being approached closely.

There are several reasons why such approaches dominate the dynamics of our system. First, due to combinatorial reasons, it is unlikely that only a single locus is polymorphic shortly after branching. As long as mutations have small phenotypic effects, one expects the polymorphism to grow initially at the same rate at every locus. To see why this is so, suppose that the initial phase of phenotypic diversification requires *n* mutations. It is much more likely that these mutations are more or less uniformly distributed over loci than that all *n* mutations occurred at the same locus. As long as *n* is large relative to the number of loci on which the ecological trait is based, it is therefore probable that the initial asymmetry between loci is small. This confines trajectories ejected from the branching point to the plane $\delta_1 = \delta_2$ (Fig. 3). Because mainly combinatorial effects determine the expected direction of evolution from the branching point, de-

tails of the mutation process can have some impact on the phase of symmetric divergence. Divergence will typically not occur at the same rate at every locus, if, for example, the mutation rate or the mutation step size is higher for some loci than for others. Similarly, convergence toward the plane $\delta_1 = \delta_2$ may either be supported or hindered by nonlinearities in the genotype-phenotype mapping.

Second, selection initially tends to decrease the average phenotypic effect of alleles, $|\bar{x}|$, thus selecting for symmetric (i.e., equal but opposite) phenotypic effects. This effect is a remnant of the regime of directional selection that drove the monomorphic population toward the evolutionary branching point: around $\delta_1 = \delta_2 = 0$, selection points toward $x = 0$ (Fig. 3). In conjunction with the first effect, this means that trajectories are ejected from the branching point in the direction $\delta_1 = \delta_2$, $\bar{x} = 0$, that is, right toward the equilibrium S2.

Finally, the closer trajectories pass by S2, the closer they will pass by S1. Because this is a derived effect, the transition from phase 3 to phase 4 will usually be less sharp than that from phase 2 to phase 3 (see Fig. 1).

Populations are thus expected to spend considerable time in the vicinity of the unstable equilibria S2 and S1. This prediction is corroborated by the individual-based simulation shown in Figure 1.

### Robustness with Respect to Genetic Assumptions

So far, we have investigated evolution under frequency-dependent disruptive selection in an idealized genetic system, characterized by free recombination and additive interactions within and between loci. In addition, we have assumed that individual mutations have small phenotypic effects. These simplifying genetic assumptions are habitually made in phenotypic models of evolution, where the details of the underlying genetics are considered to be of secondary importance (see also Weissing 1996), either because the character under study is likely to be encoded by many loci or because its genetic basis is unknown. To overcome these limitations, below we investigate the robustness of our results with respect to variations of our genetic assumptions.

#### *Genetic Linkage*

First, we consider the effects of genetic linkage between loci. Figure 4 shows numerical results for our deterministic model with tight linkage between two diallelic loci (the recombination fraction is set to $r = 0.05$).

The two loci initially behave as a single locus with four alleles (given by the haplotypes *AB, Ab, aB,* and *ab*). Based on the results presented in the preceding sections, we expect that two haplotypes disappear and that the phenotypic effects of the remaining two haplotypes evolve such that one homozygote and the heterozygote express the two locally optimal phenotypes. This is indeed the case. In the first phase of the simulation shown in Figure 4 (until about $0.5 \times 10^6$ generations), we observe the emergence of a polymorphism of five phenotypic classes, but the frequency of two of the haplotypes (*AB* and *ab*) is much higher than that of the other two haplotypes (*Ab* and *aB*). This can be inferred from the fact that the frequency of the genotypes *AAbb* and *aaBB* is much lower than that of the genotype *AaBb*. After this initial
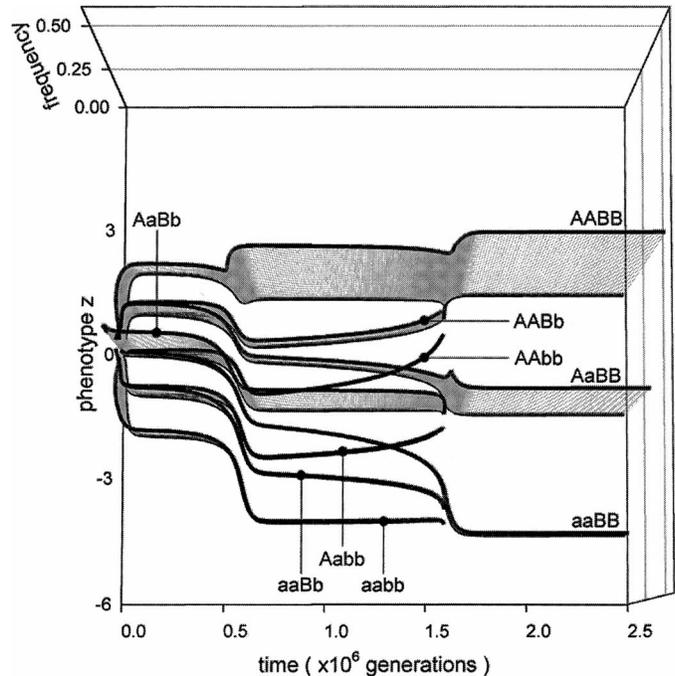


FIG. 4. Evolution with tight linkage between loci. Two tightly linked loci ($r = 0.05$), each with two alleles, behave much like a single locus with four alleles (i.e., combinations of alleles). Consequently, differentiation between loci occurs more slowly than differentiation between combinations of alleles. Parameters as in Figure 1, except $r = 0.05$.

phase, the phenotypic effect of haplotype *ab* becomes strongly negative, allowing the homozygote *AABB* and the heterozygote *AaBb* to express the two locally optimal phenotypes. Due to the tight linkage, asymmetries between the loci evolve more slowly than asymmetries between haplotypes. Eventually however, the polymorphism at one of the loci is lost. In Figure 4, the allele *b* disappears shortly after $1.5 \times 10^6$ generations.

These results suggest that linkage between loci does affect the relative rates at which asymmetries within and between loci develop, but does not change the partitioning of the evolutionary dynamics into distinguishable phases, the loss of polymorphism at all but one locus, and the final pattern of the evolutionary outcome.

#### *Nonadditive interactions*

We also consider the effects of nonadditive interactions between alleles and between loci. We could relax our assumption of additive genetics by simply imposing fixed, nonadditive interactions (e.g., antagonistic or synergistic interactions). We consider this option less than ideal, because it would still constrain the evolutionary process. Instead, we allow for evolutionary change in dominance-recessivity relations and in the relative impacts of the different loci on the phenotype (we will refer to these relative impacts as the weights of individual loci). In this extended approach, the extent to which alleles and loci contribute to the phenotype is flexible and can be shaped by evolution.

Following the modeling framework introduced by Van

TABLE 1. Dependence of the phenotype on allelic effects, allelic parameters (dominance), and modifier loci for the model variant with nonadditive interactions.

| | Locus 1 | | Locus 2 | |
|---|---|---|---|---|
| | Allele 1 | Allele 2 | Allele 1 | Allele 2 |
| Phenotypic effect | $x_{11}$ | $x_{12}$ | $x_{21}$ | $x_{22}$ |
| Allelic parameter | $u_{11}$ | $u_{12}$ | $u_{21}$ | $u_{22}$ |
| Weight of alleles | $U_{11} = u_{11}/(u_{11} + u_{12})$ | $U_{12} = u_{12}/(u_{11} + u_{12})$ | $U_{21} = u_{21}/(u_{21} + u_{22})$ | $U_{22} = u_{22}/(u_{21} + u_{22})$ |
| Alleles at modifier locus | $w_{11}$ | $w_{12}$ | $w_{21}$ | $w_{22}$ |
| Weight of loci | $W_1 = w_{11} + w_{12}/(w_{11} + w_{12} + w_{21} + w_{22})$ | | $W_2 = w_{21} + w_{22}/(w_{11} + w_{12} + w_{21} + w_{22})$ | |
| Phenotype | $z = W_1 (U_{11}x_{11} + U_{12}x_{12}) + W_2 (U_{21}x_{21} + U_{22}x_{22})$ | | | |

Dooren (1999), we implemented this flexibility by assuming that an individual's phenotype is determined by the phenotypic effects of the alleles it carries (more precisely, the gene products of the alleles) and by so-called allelic parameters, which determine the extent to which the alleles are expressed, much like regulatory elements in the promotor region of a gene. In addition, we consider modifier loci (e.g., loci coding for transcription factors) that affect the level of expression of all alleles at a given locus. Dominance interactions between alleles derive from the allelic parameters, whereas the weights of individual loci derive from the expression patterns at the modifier loci. An allele's contribution to the phenotype now depends on its weight relative to the weight of the other

allele on the same locus and on the weight of the locus relative to the weights of the other loci. This is illustrated in Table 1 for a specific example with two loci. Our approach can easily be extended to allow also for complex epistatic interactions between loci; for the sake of conciseness, we refrain from illustrating this here. We allowed both the phenotypic effects of alleles and the allelic parameters to evolve through mutations with small incremental effects. In addition, we allowed the weights of loci to evolve through mutations (again with small incremental effects) of the alleles at modifier loci (one modifier locus for each ecological trait locus). We assumed free recombination between all loci.

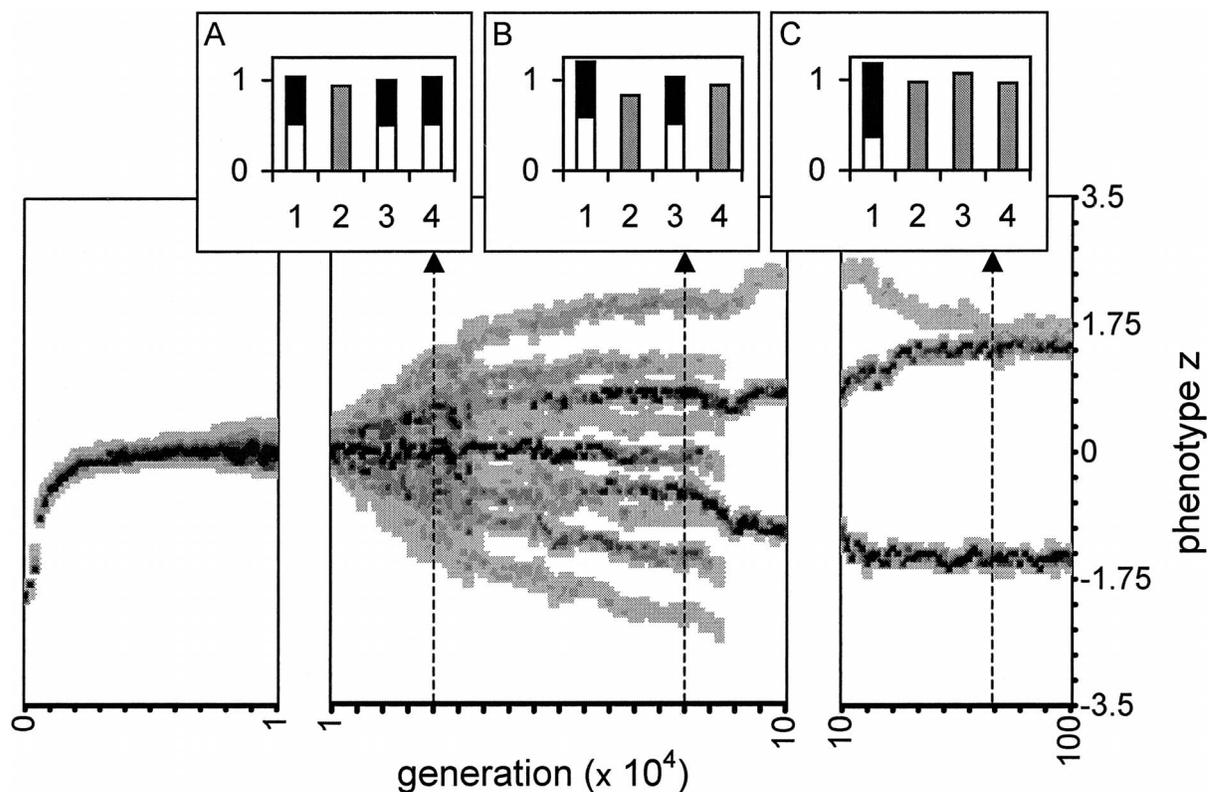Figure 5 shows numerical results for the extended indi-



FIG. 5. Evolution with variable weights for alleles and loci. Three panels show the distribution of phenotypes in an individual-based simulation as in Figure 1. The insets A–C, however, do not show frequency distributions, but the average relative weights of loci and alleles (i.e., the extent to which an allele at a specific locus contributes to the phenotype), at three moments during the simulation (indicated by dashed lines). The height of the bars represents the weight of a locus (in this simulation we kept track of four loci). For polymorphic loci, bars consist of a black and white part, indicating the weights of the different alleles that occur at this locus. Gray bars are used for monomorphic loci. Parameters as in Figure 1, except $L = 4$.
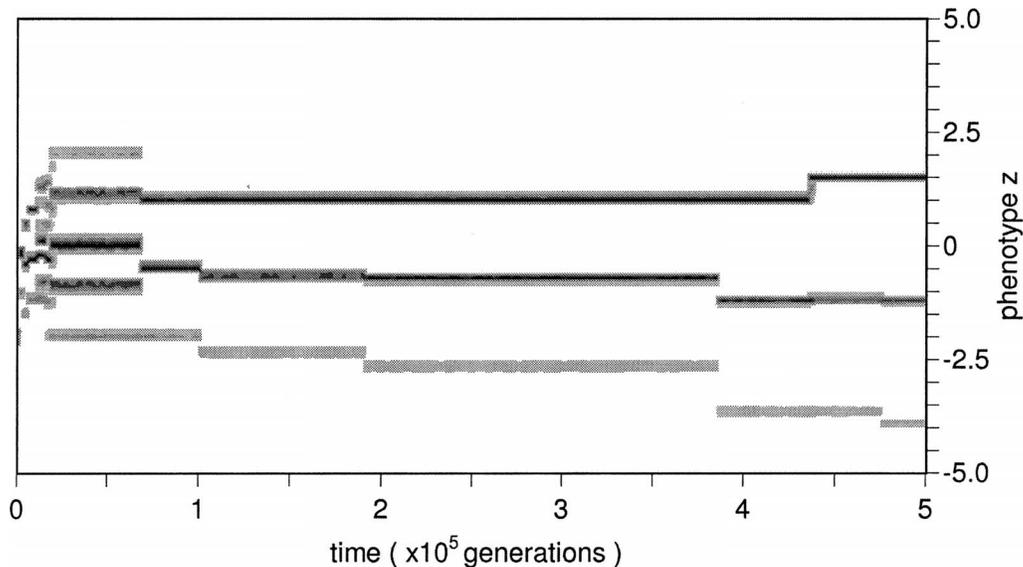
FIG. 6. Evolution with large mutational steps. Even when the whole evolutionary process is reduced to only a small number of allele substitution events, its predicted phasing is still recognizable. Parameters as in Figure 1, except $\sigma_m^2 = 0.1$ and $m = 10^{-6}$.

vidual-based model. We again observe rapid convergence to the evolutionary branching point, followed by a phase of phenotypic diversification. Initially, three of four loci become polymorphic, but eventually only one polymorphic locus remains. Insets A–C in Figure 5 show the relative weights (on the vertical axis) of the four different loci (on the horizontal axis) at three moments during the simulation. Gray bars are used for monomorphic loci; black and white bars are used for polymorphic loci. The subdivision in a white and black part represents the relative weights of the two different alleles that occur on a polymorphic locus. During the initial phase of differentiation (corresponding to phase 2 as described above), the alleles at all polymorphic loci diversify symmetrically (Fig. 5, inset A, at $3.0 \times 10^4$ generations). As long as selection favors further diversification, there is directional selection to increase the weight of polymorphic loci, which contribute to population-level phenotypic diversity, relative to the weight of the one monomorphic locus (locus 2), which does not. At this time, selection on the allelic parameters (i.e., on dominance) is still virtually absent. Later, however, the asymmetries between loci grow (corresponding to phase 3 as described above), until only one polymorphic locus remains (locus 1). During this phase, selection on the relative weights of polymorphic loci is disruptive and acts alongside selection on allelic effects (which is stabilizing for some loci but diversifying for other loci), such that the locus with the largest differentiation between alleles eventually contributes to the phenotype with the largest relative weight (Fig. 5, inset B, at $8.0 \times 10^4$ generations). All along, the interaction between alleles at a single locus has remained additive, that is, the alleles at polymorphic loci have equal relative weights. However, selection for dominance-recessivity interactions between alleles arises as soon as asymmetries evolve between alleles at the remaining polymorphic locus (corresponding to phase 4 as described above). The relative weight of one of the alleles increases, such that, eventually, the phenotype of the (otherwise) maladapted homozygote coincides with the

locally optimal phenotype matched by the heterozygote (Fig. 5, inset C, at $7.0 \times 10^5$ generations).

These results show that the evolution of nonadditive interactions between alleles and the evolution of locus weights are expected to act alongside the evolution of allelic effects, representing alternative pathways along which the symmetry between and within loci can be broken. The relative contributions of the evolution of allelic effects (the evolution of the gene products) versus the evolution of the weights of alleles and loci (the evolution of gene regulation) will depend on factors like the relative mutation rates of the phenotypic effects, the allelic parameters, and the modifier alleles. All key predictions of our preceding analysis are corroborated even in this extended model. In particular, the characteristic phasing of dynamics from the initial diversification to the final outcome is robustly recovered.

### Large Mutations

As a third check on the robustness of our results, we explore the effects of large mutational step sizes. Figure 6 shows numerical results for our original individual-based model, with all parameters except the mutational step size $\sigma_m$ and the mutation rate $m$ chosen exactly as in Figure 1. In Figure 6, the variance of mutational effects $\sigma_m^2$ was set 100 times larger than in Figure 1, and the mutation rate was set 100 times smaller, such that the expected rate of directional evolution, which scales with $m\sigma_m^2$ (Dieckmann and Law 1996; see also the appendix), was identical for both simulations.

These results show that with large mutational steps the whole evolutionary process—of convergence to the branching point, loss of polymorphism on all-but-one locus, and asymmetric differentiation of alleles at the remaining polymorphic locus—is reduced to only a small number of allele substitution events (which can be recognized individually as discontinuities in Fig. 6). Consequently, the stochasticity of the mutation process is much more pronounced, and the var-

iation between replicate simulations is larger. Yet, the average behavior of replicates does not deviate qualitatively from the predictions of our deterministic model. Also the diminished phasing of the evolutionary process is just as predicted, because smaller mutational steps make it easier for the genetic system to track the saddle connections that lie at the heart of the process. Figure 6 shows that we can still recognize the different phases discussed before, even when mutation effects are not small. It is clear that the weaker selection and the larger the mutational step size, the more strongly the stochasticity of the mutation process will blur the selection-driven, deterministic component of evolutionary change.

## DISCUSSION

Our results show that frequency-dependent disruptive selection is less powerful in maintaining polygenic variation than one would naively expect. Frequency-dependent disruptive selection does not lead to the establishment of genetic polymorphism at a large number of loci. Instead, genetic variation is concentrated at a single locus with large phenotypic effect. We observed this outcome in individual-based simulations and in an analytical model, under a range of genetic assumptions, which gives confidence in the robustness of the results. The identified pattern of polymorphism formation and collapse is likely to be widely applicable.

The dynamics observed in our model suggest a conceptual link between the different effects of frequency-dependent disruptive selection observed in quantitative genetics and adaptive dynamics models. In the initial phase of diversification, all loci are polymorphic, and the phenotypic differentiation of alleles at each locus is small. Hence, a large number of loci contribute to the genetic variation, and each locus has a small effect on the phenotype. Not surprisingly, the dynamics shortly after evolutionary branching therefore much resembles the maintenance of variation as observed in quantitative genetics models, where disruptive selection leads to the gradual broadening of a continuous phenotype distribution. Eventually, however, genetic variation becomes concentrated at a single locus, which contributes increasingly strongly to phenotypic variation. In this situation quantitative genetics methods become inaccurate: we observe the emergence of discrete clusters of phenotypes that create a situation better analyzed by adaptive dynamics methods or by classical population genetics.

The phenomena of polymorphism formation and collapse observed in our model are a straightforward consequence of the fact that frequency-dependent selection generates a dynamic selection regime. It is a defining feature of frequency dependence that the intensity and direction of selection changes as evolution proceeds, a consequence of the feedback between a population and its environment. In the context of our model, the population first experiences directional selection toward the evolutionary branching point, then disruptive selection at the branching point (leading to diversification at all loci), and subsequently again a type of stabilizing selection (favoring two discrete phenotypes at the patch optima). Selection turns from disruptive to stabilizing as soon as the phenotypic variation in the population has become large enough for the optimal phenotypes in the two patches to occur at appreciable frequencies. At that point, there is no further selection for diversification. Yet, intermediate phenotypes remain at a selective disadvantage. It is an unavoidable consequence of sexual reproduction—at least as long as individuals mate at random—that such intermediate phenotypes are generated, but, for combinatorial reasons, their frequency is lowest when all genetic variation is concentrated at a single locus. This explains why all loci, except one, eventually become monomorphic. Subsequent evolution, involving symmetry breaking between alleles at the remaining polymorphic locus, increases population mean fitness by further reducing the frequency of maladapted individuals.

Although here we have analyzed only Levene's soft-selection model, we expect that our conclusions apply to a broad class of systems subject to frequency-dependent disruptive selection. Adaptive dynamics theory has revealed the generic shape of fitness landscapes around evolutionary branching points (e.g., Geritz et al. 1997), and adaptive dynamics models have shown that such branching points can be created by a plethora of different ecological mechanisms, including all three fundamental types of ecological interaction (e.g., Doebeli and Dieckmann 2000). In particular, we expect to observe similar evolutionary phenomena in all cases where the coexistence of an arbitrarily large number of replicators is precluded by a competitive exclusion principle (Gyllenberg and Meszéna 2005). Such systems must, at some level of diversity, exhibit a transition from disruptive to stabilizing selection favoring the evolution of a discrete, limited set of phenotypes. In our Levene-type model, the number of coexisting replicators is bounded by the number of different habitats, and this sets an upper limit on the number of loci expected to remain polymorphic in long-term evolution. In a two-niche environment, at most one locus remains polymorphic. In environments with more than two habitats, polymorphism might be maintained at more than one locus (or more that two alleles might segregate at a single locus), but the number of polymorphic loci is always smaller than the number of habitat types (data available from the authors).

In a somewhat different context, Spichtig and Kawecki (2004), who recently also analyzed a multilocus version of Levene's model, came to a conclusion similar to ours. While their analysis addressed the dynamics and the equilibrium frequencies of a fixed set of alleles, other aspects of the two models are similar, allowing for a detailed comparison of results. Spichtig and Kawecki (2004) argued that the capacity of soft selection to maintain polygenic variation is smaller than one would expect based on single-locus models. Their conclusion, however, applies to parameter regimes for which evolutionary branching does not occur because the fitness of intermediate phenotypes is high. Under these conditions, polygenic variation is not maintained, due to the fact that the average phenotype of a polygenic character can be accurately matched with the optimal phenotype without requiring a polymorphism of alleles at individual loci (i.e., with all loci being homozygous, and, hence, with the population being monomorphic). This conclusion does not apply to a single locus, where the realization of an intermediary phenotype typically requires a heterozygous genotype (and, hence, a polymorphic population). Unlike for single-locus characters, the variation

of polygenic characters can therefore be low, irrespective of the mean phenotype.

In contrast, our conclusion applies to the maintenance of polygenic variation after evolutionary branching; that is, it concerns a complementary parameter regime. In this case, the explanation for the loss of polygenic variation is different and stems from the fact that a single-locus polymorphism allows for a maximal level of phenotypic variation: given a certain degree of overall differentiation between alleles, the phenotypic variance in the population is highest when the polymorphism is concentrated at a single locus. Under conditions that allow for evolutionary branching, a polymorphism of differentiated alleles at a single locus is therefore the most favorable configuration that can be attained within the limits set by sexual reproduction. It allows for the lowest possible frequency of the intermediate phenotypes that are at selective disadvantage in the parameter regime considered here.

Obviously, a single-locus polymorphism will only be favored over polygenic variation when the phenotypic effects of individual alleles are considerable, such that a polymorphism at a single locus can give rise to substantial phenotypic variation. In our model, the phenotypic effects of individual alleles can become arbitrarily large, as a cumulative result of many mutations with small phenotypic effects. In models that do not incorporate mutation, where the set of alleles is kept fixed and the phenotypic effects of individual alleles are limited, a polymorphism of alleles at a single locus can only give rise to a modest level of phenotypic variation. In such a situation, we would expect variation to be maintained at multiple loci, because this is the only way to maintain sufficient genetic variation (an expectation confirmed by Bürger 2002a,b; Spichtig and Kawecki 2004).

This highlights another contrast between our analysis and studies of frequency-dependent disruptive selection that investigate allele-frequency changes and the stability properties of population genetic equilibria of a predefined set of alleles. The latter yield conditions for the short-term maintenance of genetic variation but do not provide insights about long-term evolution, which occurs through the substitution of the existing alleles by novel, mutant alleles (Eshel 1996). This process is explicitly considered in our model. However, we have largely neglected potential constraints on the evolution of allelic effects; in the absence of knowledge that warrants more specific assumptions, we have merely assumed the mutational step size to be small. The mechanistic details of the mutation process, the development of the phenotype, and so on will be important to calibrate the different time scales of short-term and long-term evolution relative to one another. Such calibration is necessary to interpret observed patterns of polymorphism of quantitative traits in empirical systems. Conversely, a detailed comparison of these patterns to the evolutionary predictions made by short- and long-term evolution models may give insights in the importance and nature of evolutionary constraints on polygenic variation.

## Literature Cited

Abrams, P. A. 2001. Modeling the adaptive dynamics of traits involved in inter- and intraspecific competition: an assessment of three methods. Ecol. Lett. 4:166–175.

Bulmer, M. 1980. The mathematical theory of quantitative genetics. Clarendon Press, Oxford, U.K.

Bürger, R. 2000. The mathematical theory of selection, recombination and Mutation. John Wiley and Sons, Chicester, U.K.

———. 2002a. Additive genetic variation under intraspecific competition and stabilizing selection. J. Theor. Popul. Biol. 61:197–213.

———. 2002b. On a genetic model of intraspecific competition and stabilizing selection. Am. Nat. 160:661–682.

Bürger, R., G. P. Wagner, and F. Stettinger. 1989. How much heritable variation can be maintained in finite populations by mutation-selection balance? Evolution 43:1748–1766.

Caswell, H. 1989. Matrix population models. Sinauer Associates, Sunderland, MA.

Clarke, B. 1972. Density-dependent selection. Am. Nat. 106:1–13.

Cockerham, C. C., P. M. Burrows, S. S. Young, and T. Prout. 1972. Frequency-dependent selection in randomly mating populations. Am. Nat. 106:493–515.

Cressman, R. 1992. The stability concept of evolutionary game theory: a dynamic approach. Springer-Verlag, Berlin.

Dieckmann, U, and R. Law. 1996. The dynamical theory of coevolution: a derivation from stochastic ecological processes. J. Math. Biol. 34:579–612.

Doebeli, M, and U. Dieckmann. 2000. Evolutionary branching and sympatric speciation caused by different types of ecological interactions. Am. Nat. 156:S77–S101.

Eshel, I. 1996. On the changing concept of evolutionary population stability as a reflection of a changing point of view in the quantitative theory of evolution. J. Math. Biol. 34:485–510.

Felsenstein, J. 1976. The theoretical population genetics of variable selection and migration. Annu. Rev. Genet. 10:253–280.

Fisher, R. A. 1930. The genetical theory of natural selection. Oxford Univ. Press, Oxford, U.K.

Geritz, S. A. H., J. A. J. Metz, É. Kisdi, and G. Meszéna. 1997. Dynamics of adaptation and evolutionary branching. Phys. Rev. Lett. 78:2024–2027.

Geritz, S. A. H., É. Kisdi, G. Meszéna, and J. A. J. Metz. 1998. Evolutionarily singular strategies and the adaptive growth and branching of the evolutionary tree. Evol. Ecol. 12:35–57.

Geritz, S. A. H., M. Gyllenberg, F. J. A. Jacobs, and K. Parvinen. 2002. Invasion dynamics and attractor inheritance. J. Math. Biol. 44:548–560.

Gyllenberg, M., and G. Meszéna. 2005. On the impossibility of coexistence of infinitely many strategies. J. Math. Biol. 50:133–160.

Hedrick, P. W., M. E. Ginevan, and E. P. Ewing. 1976. Genetic polymorphism in heterogeneous environments. Annu. Rev. Ecol. Syst. 7:1–32.

Hofbauer, J., and K. Sigmund. 1998. Evolutionary games and population dynamics. Ch. 9: Adaptive dynamics. Cambridge Univ. Press, Cambridge, U.K.

Keightley, P. D., and W. G. Hill. 1983. Effects of linkage on re-

sponse to directional selection from new mutations. Genet. Res. 42:193–206.

Kisdi, É., and S. A. H. Geritz. 1999. Adaptive dynamics in allele space: evolution of genetic polymorphism by small mutations in a heterogeneous environment. Evolution 53:993–1008.

Levene, H. 1953. Genetic equilibrium when more than one ecological niche is available. Am. Nat. 87:331–333.

Lewontin, R. 1958. A general method for investigating the equilibrium of gene frequency in a population. Genetics 43:419–434.

Maynard Smith, J. 1982. Evolution and the theory of games. Cambridge Univ. Press, Cambridge, U.K.

Metz, J. A. J., R. M. Nisbet, and S. A. H. Geritz. 1992. How should we define ''fitness'' for general ecological scenarios? Trends Ecol. Evol. 7:198–202.

Metz, J. A. J., S. A. H. Geritz, G. Meszéna, F. J. A. Jacobs, and J. S. van Heerwaarden. 1996. Adaptive dynamics, a geometrical study of the consequences of nearly faithful reproduction. Pp. 183–231 in S. J. van Strien and S. M. Verduyn Lunel, eds. Stochastic and spatial structures of dynamical systems. Elsevier, North Holland.

Ravigné, V., I. Olivieri, and U. Dieckmann. 2004. Implications of habitat choice for protected polymorphisms. Evol. Ecol. Res. 6: 125–145.

Rifkin, S. A., D. Houle, J. Kim, and K. P. White. 2005. A mutation accumulation assay reveals a broad capacity for rapid evolution of gene expression. Nature 438:220–223.

Roughgarden, J. 1979. Theory of population genetics and evolutionary ecology: an introduction. MacMillan, New York.

Slatkin, M. 1979. Frequency- and density-dependent selection on a quantitative character. Genetics 93:755–771.

Spichtig, M., and T. J. Kawecki. 2004. The maintenance (or not) of polygenic variation by soft selection in heterogeneous environments. Am. Nat. 164:70–84.

Taylor, P. D. 1996. Inclusive fitness arguments in genetic models of behaviour. J. Math. Biol. 34:654–674.

Van Dooren, T. J. M. 1999. The evolutionary ecology of dominance-recessivity. J. Theor. Biol. 198:519–532.

Weissing, F. J. 1996. Genetic versus phenotypic models of selection: Can genetics be neglected in a long-term perspective? J. Math. Biol. 34:533–555.

Corresponding Editor: T. Hansen

APPENDIX: DERIVATION OF DETERMINISTIC APPROXIMATION

Here we derive an analytical deterministic approximation that captures the dynamics in our individual-based stochastic simulation model. To enable this complementary treatment, we assume that mutations occur rarely, such that mutant alleles arise in a resident population that is close to its population genetic equilibrium.

Consequently, a mutant allele interacts only with the currently predominant resident alleles, which were successful at ousting previous mutant alleles. We also assume that the population is sufficiently large, such that we may neglect stochasticity in the dynamics of the frequencies of resident alleles, and that changes in the phenotypic effects of alleles caused by individual mutations are typically small, such that it is meaningful to approximate the long-term dynamics of phenotypic effects deterministically.

The invasion fitness $\lambda$ specifies the geometric rate of increase of the abundance of a mutant allele while it is rare (e.g. just after it has arisen by mutation; Metz et al. 1992, 1996). When a mutant arises in an otherwise genetically monomorphic resident population, all resident individuals have the same phenotype $\hat{z}$ and all individuals that carry a mutant allele have the same phenotype $Z$. This greatly simplifies the derivation of invasion fitness in our model (e.g., Kisdi and Geritz 1999), which under such conditions is given by

$$\lambda = \frac{1}{2}[v_1(z)/v_1(\hat{z}) + v_2(z)/v_2(\hat{z})]. \qquad (A1)$$

The first and second term in the square bracket represent, respectively, the relative viabilities of mutant individuals in the first and second habitat, and the factor ½ simply reflects the assumption that half of the individuals in the mating population are recruited from either habitat.

When the resident population is polymorphic at one or more loci, the derivation of invasion fitness becomes more complicated, because we then need to keep track of the frequencies of the different resident genotypes. The mutant allele may then also occur in different genetic backgrounds, consisting of different combinations of resident alleles. To keep the analysis tractable, we will restrict ourselves here to the simplest interesting case, by considering a resident population that is polymorphic at two loci ($L = 2$). We denote the alleles at the first locus by $A$ and $a$, and the alleles at the second locus by $B$ and $b$ (as mentioned in the main text, this notation does not imply that the alleles $A$ and $B$ are dominant). The phenotypic effects of the alleles are denoted by $x_A$, $x_a$, $x_B$, and $x_b$. If $x_A = x_a$ or $x_B = x_b$, the resident population is monomorphic at the corresponding locus. We also consider a mutant allele $M$, with phenotypic effect $x_m$, that has arisen through mutation of the allele $A$ at the first locus (other mutant alleles are dealt with analogously).

We choose to describe the dynamics of the resident and mutant allele frequencies in terms of the frequencies of the haploid gametes in which they occur: $f_g$ denotes the frequency of the gamete $g$ ($g = AB, Ab, aB, MB$, or $Mb$) in adults at the moment of reproduction, that is, after viability selection has occurred. We follow the life cycle of our model to determine its effect on these gamete frequencies.

*Random mating.*—We first compute the frequency $F'_{gg'}$ of the genotype $gg'$ in the offspring before viability selection. Because mating is random, the frequency of offspring carrying the genotype $gg'$, which arises from the combination of gametes $g$ and $g'$ is given by the product of the corresponding gamete frequencies in the parents, $F'_{gg'} = f_g f_{g'}'$.

*Viability selection.*—Viability selection changes the genotype frequencies in the offspring, such that the frequency $F_{gg'}$ of the genotype $gg'$ after viability selection is, similarly to equation (A1),

$$F_{gg'} = F'_{gg'}\frac{1}{2}[v_1(z_{gg'})/\bar{v}_1 + v_2(z_{gg'})/\bar{v}_2], \qquad (A2)$$

where $Z_{gg'}$ denotes the phenotype encoded by the genotype $gg'$ (e.g., $Z_{ABAb} = 2x_A + x_B + x_b$ and $Z_{abMb} = x_a + x_M + 2x_b$) and $\bar{v}_i$ is the average viability in habitat $i$. While the mutant allele is rare, average viabilities do not depend on the mutant's genotype frequencies,

$$\bar{v}_i = \sum_{g,g'=AB,Ab,aB,ab} F'_{gg'}v_i(z_{gg'}). \qquad (A3)$$

*Gamete production.*—After viability selection, the next generation is produced through sexual reproduction. The frequencies of the different resident gametes are determined straightforwardly from the resident genotype frequencies after viability selection. For example,

$$f_{AB} = F_{ABAB} + \frac{1}{2}\sum_{g=Ab,aB}(F_{ABg} + F_{gAB})$$
$$+ \frac{1}{2}(1-r)(F_{ABab} + F_{abAB}) + \frac{1}{2}r(F_{AbaB} + F_{aBAb}), \qquad (A4)$$

where $r$ is the coefficient of recombination between the two loci. The mutant's genotype frequencies do not appear in equation (A4), since the frequency of the mutant allele is initially negligible.

Equations (A2) to (A4) define a recurrence relation for the resident gamete frequencies. This recurrence relation can be iterated until these frequencies converge to a stable equilibrium (reflecting our assumption that resident populations attain their population genetic equilibrium by the time a mutant arises).

For the mutant gamete frequencies we obtain, analogously to equation (A4),

$$f_{MB} = \frac{1}{2} \sum_{g=AB,aB} (F_{MBg} + F_{gMB})$$

$$+ \frac{1}{2}(1 - r) \sum_{g=Ab,ab} (F_{MBg} + F_{gMB})$$

$$+ \frac{1}{2}r \sum_{g=AB,aB} (F_{Mbg} + F_{gMb}),$$

$$f_{Mb} = \frac{1}{2} \sum_{g=Ab,ab} (F_{Mbg} + F_{gMb})$$

$$+ \frac{1}{2}(1 - r) \sum_{g=AB,aB} (F_{Mbg} + F_{gMb})$$

$$+ \frac{1}{2}r \sum_{g=Ab,ab} (F_{MBg} + F_{gMB}). \tag{A5}$$

Here we again use the fact that the mutant allele is rare initially, which allows us to neglect the frequency of individuals that are homozygous for the mutant allele.

For mutant alleles $M$ that differ only slightly from the resident allele $A$, $|x_M - x_A|$ is small, and we may use first-order Taylor expansions to approximate the viabilities of phenotypes affected by the mutant allele. For example,

$$v_i(z_{MBg}) = \exp\left[-\frac{1}{2}(z_{MBg} - \mu_i)^2/\sigma^2\right]$$

$$\approx [1 - (x_M - x_A)(z_{ABg} - \mu_i)/\sigma^2]v_i(z_{ABg}). \tag{A6}$$

Using these approximations and equation (A2), we rewrite the mutant genotype frequencies. For the mutant genotype frequencies $F_{MBg}$, for example, this yields

$$F_{MBg} = \frac{f_{MB}}{f_{AB}}F_{ABg} + f_{MB}(x_M - x_A)W_g^{AB}, \tag{A7}$$

where

$$W_g^{g'} = -\frac{1}{2}f_g\sigma^{-2}[(z_{gg'} - \mu_1)v_1(z_{gg'})/\bar{v}_1$$

$$+ (z_{gg'} - \mu_2)v_2(z_{gg'})/\bar{v}_2]. \tag{A8}$$

We substitute equation (A7) and analogous expressions for the genotype frequencies $F_{gMB}$, $F_{Mbg}$, and $F_{gMb}$ into equations (A5), to obtain, after some rearrangement, the following recurrence relation for the change of mutant gamete frequencies from one generation to the next,

$$\begin{pmatrix} f_{MB} \\ f_{Mb} \end{pmatrix} \to [\mathbf{F} + (x_M - x_A)\mathbf{W}]\begin{pmatrix} f_{MB} \\ f_{Mb} \end{pmatrix}, \tag{A9}$$

where the matrices $\mathbf{F}$ and $\mathbf{W}$ are defined as

$$\mathbf{F} = \begin{bmatrix} 1 - rf_{AB}^{-1}(F_{ABAb} + F_{AbaB}) & rf_{Ab}^{-1}(F_{ABAb} + F_{AbaB}) \\ rf_{AB}^{-1}(F_{ABAb} + F_{ABab}) & 1 - rf_{Ab}^{-1}(F_{ABAb} + F_{ABab}) \end{bmatrix}, \tag{A10}$$

$$\mathbf{W} = \begin{bmatrix} \sum_{g=AB,aB} W_g^{AB} & r \sum_{g=AB,aB} W_g^{Ab} \\ + (1-r)\sum_{g=Ab,ab} W_g^{AB} & \\ r \sum_{g=Ab,ab} W_g^{AB} & \sum_{g=Ab,ab} W_g^{Ab} \\ & + (1-r)\sum_{g=AB,aB} W_g^{Ab} \end{bmatrix}. \tag{A11}$$

The invasion fitness $\lambda$ of the mutant allele in the considered polymorphic resident background is now given by the geometric rate of increase of the mutant allele frequency, which equals the dominant eigenvalue of the matrix $\mathbf{F} + (x_M - x_A)\mathbf{W}$. For small $|x_M - x_A|$ it can be shown (e.g., Caswell 1989; Taylor 1996) that

$$\lambda = 1 + (x_M - x_A)\frac{v\mathbf{W}u}{vu}. \tag{A12}$$

The term $v\mathbf{W}u/(vu)$, which represents the fitness gradient, varies with the vectors

$$v = (F_{ABAb} + F_{ABab}, F_{ABAb} + F_{AbaB}) \quad \text{and} \tag{A13a}$$

$$u = \begin{pmatrix} f_{AB} \\ f_{Ab} \end{pmatrix}, \tag{A13b}$$

which are the dominant left and right eigenvectors of the matrix $\mathbf{F}$, respectively. Under suitable assumptions (Dieckmann and Law 1996; Weissing 1996; Hofbauer and Sigmund 1998), the invasion fitness can be used to describe the long-term rate and direction of a series of allelic substitution events. Indeed, using equation (A12) and following the derivation scheme employed by Dieckmann and Law (1996), it can be shown that the expected evolutionary rate of change of the phenotypic effect of the currently resident allele $A$ at the first locus satisfies

$$\frac{dx_A}{dt} = \int 2Nm(f_{AB} + f_{Ab}) \cdot M(x_M | x_A)$$

$$\times \alpha \max\left[0, (x_M - x_A)\frac{v\mathbf{W}u}{vu}\right] \cdot (x_M - x_A) \, dx_M, \tag{A14}$$

where $t$ measures evolutionary time in generations. The first factor in the integrand above is the rate at which new mutant alleles arise: the frequency of allele $A$ is given by $f_{AB} + f_{Ab}$, the total number of alleles in a diploid population of size $N$ is $2N$, and $m$ equals the mutation rate per generation. The second factor is the probability density according to which a mutation changes the phenotypic effect at the first locus from $x_A$ to $x_M$. The third factor is the probability that the mutant allele will successfully invade. This probability is zero when the mutant allele has a geometric rate of increase below that of the resident allele and otherwise is proportional to the fitness advantage $s$ of the mutant allele, as long as $s$ is small. This explains the function $\alpha \max(0, s)$, with $\alpha$ denoting the constant of proportionality, and with $s = (x_M - x_A)(v\mathbf{W}u)/(vu)$ following from equation (A12). For offspring numbers varying according to a Poisson distribution, we obtain $\alpha = 2$. If the mutant allele succeeds to invade, this causes a change of the resident allele: away from the evolutionary branching point (and from population dynamical bifurcation points), successful invasion of the mutant allele implies that it will eventually replace the resident allele (Geritz et al. 2002). Successful invasion thus means that the phenotypic effect of the currently resident allele will change by an amount $x_M - x_A$, which explains the integrand's fourth factor.

Collecting all terms that are independent of $x_M$ in front of the integral, and realizing that the integrand above vanishes along half its range because only mutant alleles with either $x_M > x_A$ or $x_M < x_A$ can successfully invade, we can rewrite equation (A14) as

$$\frac{dx_A}{dt} = 2Nm(f_{AB} + f_{Ab})\alpha\frac{v\mathbf{W}u}{vu}$$

$$\times \frac{1}{2}\int (x_M - x_A)^2 M(x_M | x_A) \, dx_M. \tag{A15}$$

Denoting the variance of mutational effects by $\sigma_m^2$, we therefore finally obtain

$$\frac{dx_A}{dt} = Nm\alpha\sigma_m^2(f_{AB} + f_{Ab})\frac{v\mathbf{W}u}{vu}. \tag{A16}$$

Equations for the rate of change in the phenotypic effects of the alleles $a$, $B$, and $b$, are derived analogously.